

## AN RFQ BASED NEUTRON SOURCE FOR BNCT\*

X. W. Zhu<sup>†</sup>, Z. Y. Guo, Y. R. Lu<sup>#</sup>, H. Wang, Z. Wang, K. Zhu, Y. B. Zou  
 State Key Lab Nuclear Physics and Technology  
 Peking University, Beijing 100871, China

### Abstract

Boron Neutron Capture Therapy (BNCT) [1, 2], promises a bright prospect for future cancer treatment, in terms of effectiveness, safety and less expense. The PKU RFQ group proposes an RFQ based neutron source for BNCT. A unique beam dynamics design of 162.5 MHz BNCT-RFQ, which accelerates 20 mA of H<sup>+</sup> from 30 keV to 2.5 MeV in CW operation, has been performed in this study. The Proton current will be about 20 mA. The source will deliver a neutron yield of  $1.76 \times 10^{13} \text{ n/sec/cm}^2$  in the  ${}^7_3\text{Li}(p, n){}_4^7\text{Be}$  reaction. Detailed 3D electromagnetic (EM) simulations of all components, including cross-section, tuners, pi-rods, and cut-backs, of the resonant structure are performed. The design of a coaxial type coupler is developed. Two identical RF couplers will deliver approximately 153 kW CW RF power to the RFQ cavity. RF property optimizations of the RF structures are performed with the utilization of the CST MICROWAVE STUDIO [3].

### BEAM DYNAMICS

BNCT treatment requires sufficient fluxes of thermal (< 0.5 eV) or epithermal (0.5 eV ~ 10 keV) neutrons for its application. The 4-vane proton RFQ will accelerate a 15 mA beam to 2.5 MeV at 162.5 MHz in CW operation for safety margin, and it is also demanded that the design should keep high transmission up to 20 mA.

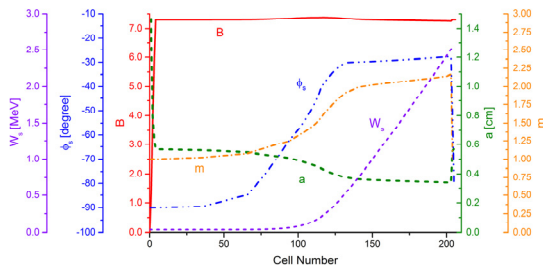


Figure 1: Main parameters of the BNCT RFQ beam dynamics.

The beam dynamics design of BNCT RFQ adopts the New Four-Section Procedure (NFSP) design strategy [4], and the main design parameters are shown in Fig. 1.

Based on the PARMTEQM code [5],  $10^5$  input macro particles are put into the multiparticle dynamics simulations. Fig. 2 shows the simulation results at 20 mA.

Table 1 summarizes the detailed simulation results, where the Kilpatrick factor is only 1.24, quite reliable for CW operation. The modest inter-vane voltage is kept constant at 65 kV, and does bring benefits to ease the

thermal management, which the bottleneck in CW RFQ operation. The transverse focusing strength B is kept constant to simplify the cross-section design, which makes it easier to tune the cavity, and constant transverse radius of curvature allows to machine the vanes with flying cut. The design has a transmission of 99.6% at 20 mA. However, even at 40 mA, which is twice as large as the design value, the transmission is still as high as 96.6%. Tolerance analyses have been completed; the analyses indicate the RFQ design well tolerates the twiss parameters, mechanical and field errors.

Clearly, the design and simulation results satisfy all requirements well for the BNCT RFQ.

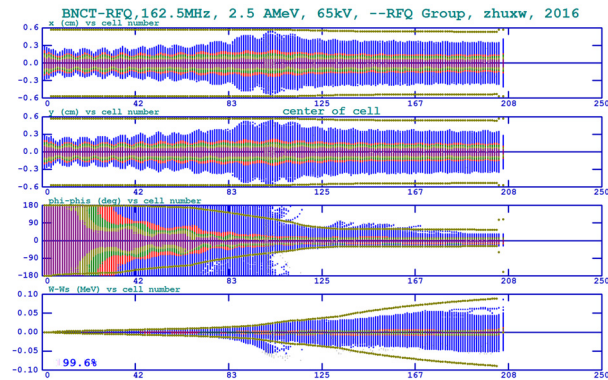


Figure 2: PARMTEQM simulations of the RFQ at 20 mA.

Table 1: RFQ Parameter List

BNCT RFQ	Value
Input energy	35 keV
Output energy	2.5 MeV
Frequency	162.5 MHz
DC current	20 mA
Vane voltage	65 kV
Vane length	523.4 cm
RF power (PEC)	103 kW
Beam Power	50 kW
$\epsilon_t$ (norm. rms, exit)	0.25 mm mrad
$\epsilon_l$ (norm. rms, exit)	0.0655 MeV deg
$E_{s,max}/E_k$	1.24

### RF STRUCTURE

The RFQ resonator design aims to satisfy the requirements given by beam dynamics. These studies involves iteration of RF electromagnetic simulations to provide good mode stabilization, right operating frequency, and coupling. Both 2D SUPERFISH code and CST MICRO-

\* Work supported by 2014CB845503

<sup>†</sup> zhuxw13@pku.edu.cn

<sup>#</sup> yrlyu@pku.edu.cn

WAVE STUDIO are used to design and optimize the cross-section. With great development in computation capability, the 3D CST MWS is capable of resolving the complexity of the RFQ structure. Detailed RF modelling on the BNCT RFQ resonator structure including pi-mode stabilizer rods, tuners, cut-backs (at entrance and exit) and radial matching section, have been taken into account. Due to CW operation, power loss on each component of the resonator is an important parameters for thermal management, and careful attention and efforts have been paid to dealing with it correctly.

### Cross-section Design

Figure 3 shows the final RFQ cross-section design simulated with CST MWS. In the following simulations, only parameter  $H$ , half of the inner width of the RFQ, was used to tune the operating frequency, and the black arrow denotes it was a geometry variable in the optimization process. Here parameter  $H$  equals to 176.911 mm.

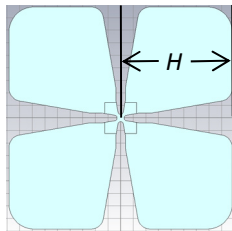


Figure 3: Cross-section of BNCT RFQ.

### Pi-mode Stabilizer Period and Tuner Period

Tuning and field stabilizing elements were studied with periods of the RFQ. The lengths of periods are defined by element spacing along RFQ. To calculate the power dissipation of each element, the field strength in the RFQ periods has been always scaled to 65 kV.

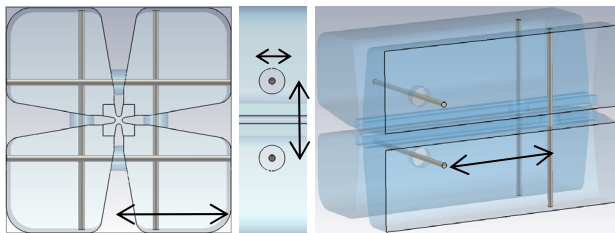


Figure 4: The pi-mode stabilizer period.

Aiming to attain the field stabilization along the RFQ, 20 pairs of water-cooled pi-rods, in Fig. 4, are installed to efficiently separate the unwanted dipole mode ( $D_0$ ) from the quadrupole mode ( $Q_0$ ). With or without the PISL, the mode separations are 5.0053 MHz and 19.0520 MHz, respectively. And the Q value goes down 9.75% from 16896. After optimization, the pi-rods have outer diameter of 10 mm and pass through 40 mm holes in the vanes.

The total 100 slug tuners are integrated into the RFQ cavity, and each tuner, shown in Fig. 5, has an outer diameter of 60 mm and 20 mm nominal intrusion. Simulations of a tuner period give a tuning range of 1.4056 MHz, with a tuning sensitivity of 17.57 kHz/mm.

The maximum local frequency shift results from the modulation was found to be 397 kHz in a cell length with

a modulation factor of 2.237, which can be made up by plug tuners with sufficient margins. Consequently, it was decided to continue design with flat vane tips (Fig. 6).

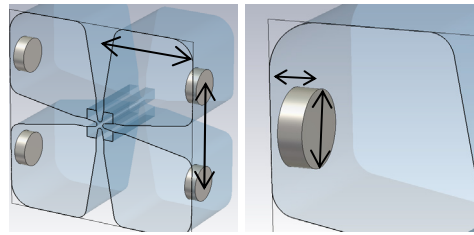


Figure 5: The tuner period.

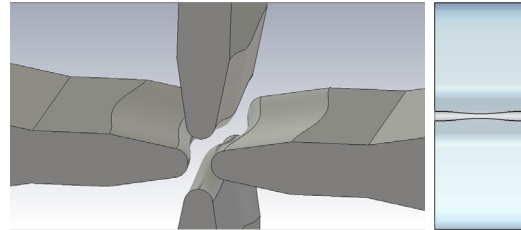


Figure 6: Unit cell with maximal vane tip modulation.

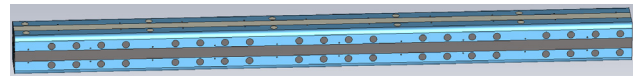


Figure 7: Main body tuning with PISLs and tuner periods.

There does not exist a regular period of the structure, which can sufficiently describe effects with combined rods and tuners. This is because pi-rods and slug tuner have different spacing. So a vane length model in 5200 mm length, in Fig. 7, comprised of 100 tuners and 20 pairs of pi-rods, and with perfect magnetic boundary conditions at both ends, has been taken into account. The final tuning of the RFQ main body was performed and the tuning parameter  $H=172.660$  mm was fixed.

### Cut-back Tuning

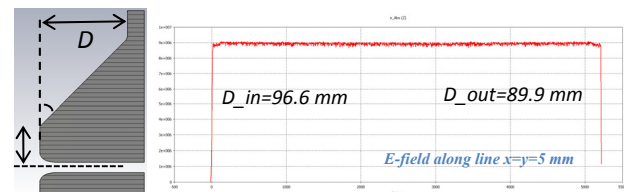


Figure 8: Cut-back tuning and field flatness.

Field flatness is always one of the most important tasks in RFQ design and tuning, and is of considerable sensitivity with the cut-back dimensions. Due to mechanical and manufacturing preference, a triangle shape of cut-backs, in Fig. 8, is determined.

The tuning depth  $D$ , is the most influential parameter, and a full model with complete sets of solid components, has been performed to tune the field, and provides an opportunity to evaluate the RF power losses on the parts separately. This gives the opportunity to develop cooling scheme in future, and helps to pay attention to the most critical part in terms of power density.

In Table 2, the power dissipation values for separate parts of the RFQ are summarized. In the numerical simu-

lations above, the perfect conducting ( $5.8 \times 10^7 S/m$ ) and contacts between separate parts are assumed. Depending on the quality of the copper and brazing, the real total power losses are expected to be higher up to 20% [6].

Table 2: Power Dissipations on Separate Parts of BNCT RFQ

Part	Total, kW	%
Walls	40.72	39.5
Vanes, 4 units	42.57	41.3
Input cut-backs, 4 units	1.86	1.8
Output cut-backs, 4 units	2.02	2.0
Pi-rods, 40 units	8.59	8.3
Tuners, 100 units	7.38	7.2
Total	103.14	100

### RF COUPLER DESIGN

The total power of 153 kW, including 103 kW for cavity loss and 50 kW for beam loading respectively, will be coupled into the BNCT RFQ cavity. And the coupling factor is 1.5. Two identical couplers will be equipped with the RFQ cavity, to ease the coupler power demands and maintain a reliable operation. Compared with the Iris type coupler, the coaxial loop couplers are preferred, with benefits in easily adjusting the coupling factor and modifying the multipacting power level. The outer conductor is a standard 3-1/8" coaxial transmission line, and the input impedance is 50 Ohm.

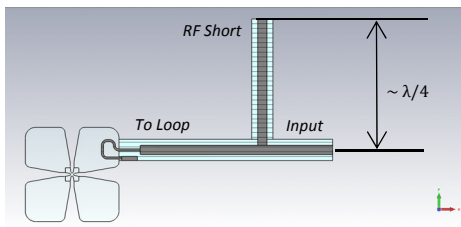


Figure 9: Sectional view of a quarter-wave stub and loop inside the RFQ cavity.

In Fig. 9, the RF structure of a quarter-wave stub is shown. It provides a convenient way of accessing the inner conductor with water cooling, and matching a load to a source by introducing an intentional reflection.

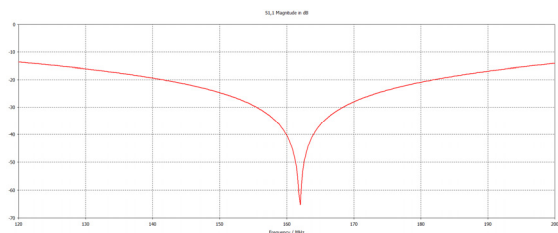


Figure 10: Passband of a quarter wave stub.

By tuning the height of the stub, it is easy to reduce the reflection. Given in Fig. 10, the coupler has a rather wide passband, and the reference coefficient of S11 is -65 dB at 162.5 MHz. Here the bandwidth is approximately 40 MHz, which refers to the return loss is below -20 dB.

The effective area of the loop, shown in Fig. 9, can be estimated by a lumped circuit [7]. And the coupling can be adjusted by loop rotation. It is good to design the couplers to have a total beta of slightly greater than one, which will also take into account the beam loading. In Fig. 11, the smith chart shows the S11 of the input coupler.

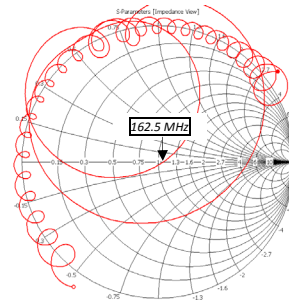


Figure 11: Smith chart shows the S11 of input coupler.

The power sources, such as a solid state RF amplifier [8], a tetrode-based (TH781) RF transmitter [9] and the Thales diacode (TH628) [9], will be considered for this application.

### CONCLUSION

The beam dynamics design of 162.5 MHz BNCT-RFQ, which accelerates 20 mA of H+ from 30 keV to 2.5 MeV in CW operation, is completed and frozen. The RF EM design is also complete, including RF structure and terminations. The input power coupler design and simulations are in processing.

### REFERENCES

- [1] M. Yoshioka, in *Proc. IPAC'16*, pp. 3171-3175.
- [2] Barth, Rolf F., et al. "Current status of boron neutron capture therapy of high grade gliomas and recurrent head and neck cancer." *Radiation Oncology* 7.1 (2012): 1.
- [3] CST Simulation packages, <http://www.cst.com>.
- [4] C. Zhang *et al.*, "Beam dynamics studies on a 200mA proton radio frequency quadrupole accelerator," *Nucl. Instr. Meth.*, vol. 582, pp. 153-159, 2008.
- [5] K.R. Crandall, LANL Internal Report, Nr. LA-UR-96-1836, Revised December 7, 2005.
- [6] G. Romanov, in *Proc. IPAC'12*, pp. 3883-3885.
- [7] Kondo, Yasuhiro, et al. "Design of an RF coupler for the J-PARC RFQ.", *Proceedings of Particle Accelerator Society Meeting 2009*, JAEA, Tokai, Naka-gun, Ibaraki, Japan.
- [8] SigmaPhi, <http://www.signaphi.fr/rf-transmitters.html>.
- [9] THALES, <https://www.thalesgroup.com/>.